

Photoemission spectra and band structures of *d*-band metals. VIII. Normal emission from Cu(111)

N. V. Smith

Bell Laboratories, Murray Hill, New Jersey 07974

R. L. Benbow and Z. Hurych

Department of Physics, University of Northern Illinois, DeKalb, Illinois 60115

(Received 14 November 1979)

The normal photoemission spectra from Cu(111) have been calculated using a simple bulk-band-structure model. Momentum matrix elements are included and are calculated from the k -space derivatives of a combined-interpolation-scheme Hamiltonian. For s -polarized light the results are in excellent agreement with the recent experimental results of Knapp *et al.* For p polarization, agreement is obtained only after an artificial suppression of the relative intensity of the perpendicular component of the electromagnetic field by a factor of ~ 5 . It is suggested that this suppression arises through local-field effects in the vicinity of the surface.

I. INTRODUCTION

The strong relationship between photoemission spectra and bulk-band structures is well known and forms the basis of the three-step model of the photoemission process.¹ The theme of this series of papers^{2,3} has been to establish and to explore the limits of this relationship using a combined-interpolation-scheme approach. In this paper we examine the extent to which bulk-band theory can account for the intensities in angle-resolved photoemission experiments on Cu. We concentrate specifically on the normal emission spectra from Cu(111) which have been measured recently by Knapp, Himpfel, and Eastman⁴ (KHE) using synchrotron radiation. We employ the computational scheme described in the preceding paper of the series³ (referred to hereafter as VII) to calculate the energy bands and momentum matrix elements for optical transitions. The calculational details are set out in Sec. II. The results for Cu(111) are presented and compared with experiment in Sec. III. In order to obtain a reasonable match between theory and experiment, it was found necessary to introduce an artificial suppression of the component of the electromagnetic vector potential perpendicular to the surface relative to the component parallel to the surface. This is discussed in Sec. IV.

II. NUMERICAL METHOD

The key ingredient in this work is the use of the expression which relates the momentum operator for Bloch wave functions to k -space derivatives of the Hamiltonian⁵:

$$\vec{P} = \frac{m}{\hbar} \frac{\partial H(\vec{k})}{\partial \vec{k}}. \quad (1)$$

In the combined-interpolation-scheme approach, H is expressed explicitly in terms of simple analytic functions of \vec{k} . The momentum matrix elements are then readily obtained without the need to introduce any additional disposable parameters. It was shown in VII that this approach yields theoretical results for ϵ_2 , the imaginary part of the dielectric function, which are competitive with those obtained by first-principles calculations. Results were also presented in VII for the momentum matrix elements for optical transitions along the ΓL direction in k space; these are shown in Fig. 1. These results are appropriate to normal photoemission from Cu(111) in the photon-energy range $\hbar\omega \lesssim 25$ eV. The form of the results has been discussed in VII. In particular, the momentum matrix element \vec{P}_{fi} is parallel (perpendicular) to the [111] direction for the Λ_1 (Λ_3) bands.

To convert results such as those in Fig. 1 to actual spectra, we use the standard expression for the angle-resolved photoemission spectrum within the three-step model⁶:

$$N(E, \hbar\omega, \vec{K}_\parallel) \propto \sum_{fi} \int d^3k |\vec{A} \cdot \vec{P}_{fi}|^2 D(E_f, \vec{k}) T(E_f, \vec{k}_\parallel) \\ \times \delta(E - E_f) \delta(E_f - E_i - \hbar\omega) \\ \times \delta(\vec{K}_\parallel - \vec{k}_\parallel - \vec{G}_\parallel). \quad (2)$$

$E_f(\vec{k})$ and $E_i(\vec{k})$ represent energy eigenvalues at \vec{k} in final band f and initial band i , respectively; \vec{K} is the external wave vector of the photoemitted electron, \vec{A} is the vector potential of the electromagnetic field, and $D(E_f, \vec{k})$ and $T(E_f, \vec{k}_\parallel)$ are factors which account, respectively, for the probabilities that the photoexcited electron arrives at the surface without inelastic scattering, and then

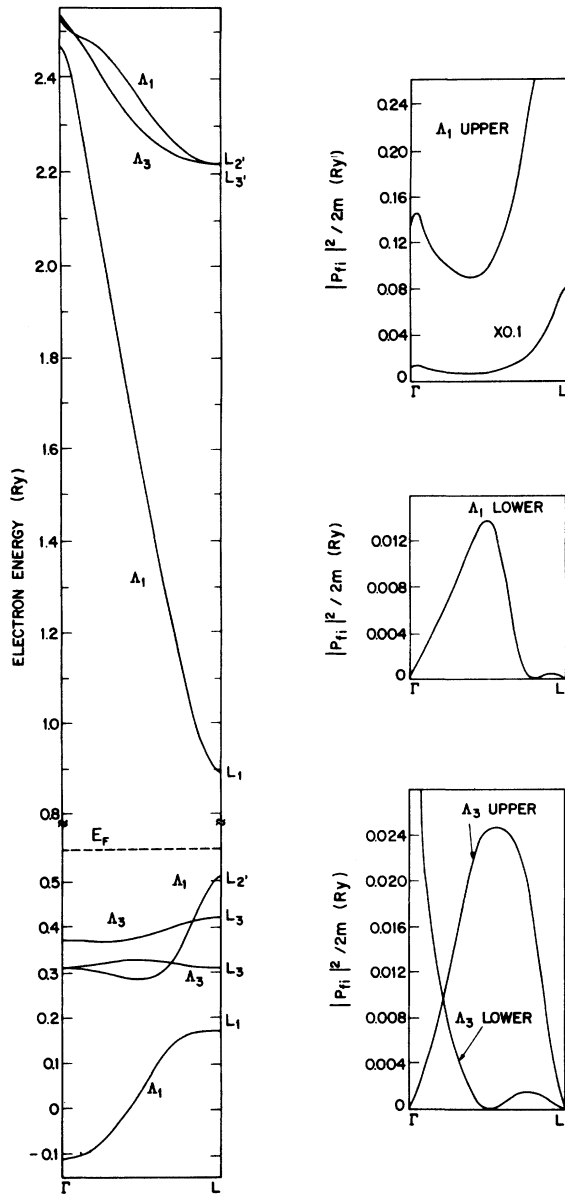


FIG. 1. Band structure and momentum matrix elements for Cu along the [111] direction. The panels on the right show the dependence of $|P_{fi}|^2/2m$ with perpendicular wave vector k_{\perp} for transitions from the initial-state bands indicated to final states in the lower unoccupied Λ_1 band. For Λ_1 (Λ_3) initial states \vec{P}_{fi} is parallel (perpendicular) to the [111] direction.

escapes across it. In the case of normal emission from Cu(111), the k -space integral of Eq. (2) need be conducted only along the ΓL line, and only $\vec{G}_{\parallel} = 0$ need be considered. As further simplifications, we treated D as constant; T was set equal to zero for values of E_f less than the vacuum level (taken at 4.7 eV above the Fermi level), and was treated as constant otherwise. These are approxi-

mations which can be readily refined in the future if desired. Our calculations, therefore, place emphasis on the role of $|P_{fi}|^2$ in determining the relative peak intensities in the spectra.

The actual computations were performed by diagonalizing H at about 200 points distributed uniformly along the ΓL line. Spectra at specific photon energies were then obtained by interpolation using a prescription for lifetime broadening essentially the same as that proposed by KHE.⁴ The final results were given a further smoothing by convoluting with a Gaussian with a FWHM of 0.35 eV to simulate the instrumental resolution function.

Polarization effects are clearly embodied in Eq. (2) through the vector \vec{A} , which we resolve in the usual way into its s and p components \vec{A}_s and \vec{A}_p . In the case of s polarization, \vec{A}_s is perpendicular to [111], so only the initial states of Λ_3 symmetry can be excited. For p polarization, \vec{A}_p has components perpendicular and parallel to the surface which we shall denote by $\vec{A}_{p\perp}$ and $\vec{A}_{p\parallel}$; these will excite, respectively, the Λ_1 and Λ_3 states. To compute their relative strengths we must make some provision for the value of $|A_{p\perp}/A_{p\parallel}|$. It is convenient to introduce the quantities for the outside and inside, respectively,

$$\xi_i \equiv |A_{p\perp}/A_{p\parallel}|^2, \quad (3)$$

$$\xi_t \equiv |A_{p\perp}/A_{p\parallel}|^2,$$

where the subscripts i and t refer to the incident and transmitted electromagnetic fields. It turns out that for Cu in the energy range of interest here, we have $\xi_t \ll \xi_i$. Part of this suppression can be accounted for by the macroscopic optical constants, but a large part cannot. For the immediate purposes of calculating spectra, we have treated ξ_t as disposable. In an unadulterated three-step approach based upon a bulk-band model it is, of course, the internal value ξ_t rather than the external value ξ_i which is applicable. We shall return to this topic in Sec. IV.

III. RESULTS

A. General

As an example of the data of KHE, Fig. 2 shows a normal emission photoelectron energy spectrum taken on Cu(111) at $\hbar\omega = 10.5$ eV. Intense emission is observed from a surface state just below the Fermi level E_F ; this will not concern us further here since it is beyond the scope of a purely bulk-band-structure model. Our interest centers on the emission from the bulk bands in the energy region -4 to -2 eV. After subtraction of the inelastic background, this bulk emission is shown

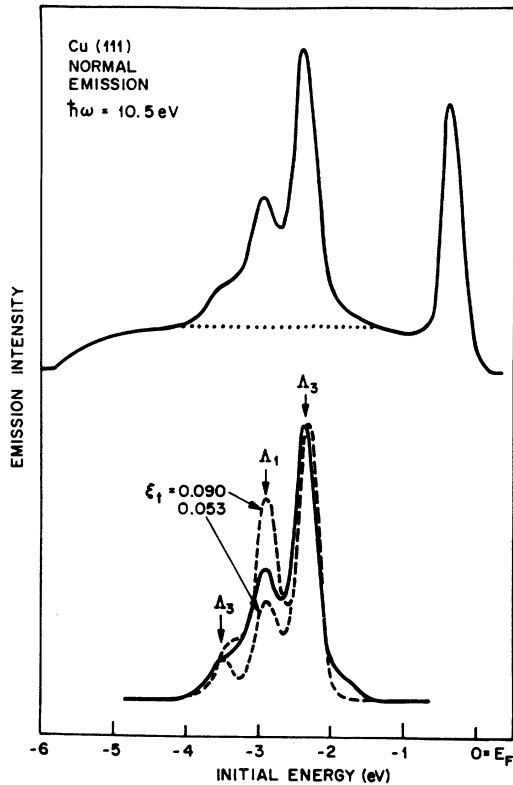


FIG. 2. Normal photoemission spectrum from Cu(111) for p -polarized light with $\hbar\omega = 10.5$ eV. The upper full curve is the experimentally measured spectrum of KHE (Ref. 4). The lower full curve represents the experimental data in the bulk-band-structure region after subtraction of the inelastic background (dotted line in upper part of figure) and removal of the surface-state emission from just below the Fermi level. The dashed curves are theoretically calculated spectra for two different values of $\xi_i \equiv |A_{p\perp}/A_{p\parallel}|^2$.

at the full curve in the lower part of Fig. 2.

For the measurements of Fig. 2 the incident radiation was p polarized so that both Λ_1 and Λ_3 symmetry states could be excited. Their relative strengths will depend on the relative values of $|A_{p\perp}|^2$ and $|A_{p\parallel}|^2$, respectively. The quoted angle of incidence⁷ was $\theta_i = 60^\circ$, so that we have $\xi_i = 3.0$ and $\xi_i = 0.45$ (see Sec. IV). This value of ξ_i would predict a much larger intensity of the Λ_1 emission relative to the Λ_3 emission than is actually observed. We have, therefore, used ξ_i as disposable. The dashed curves in Fig. 2 show the theoretically calculated spectra (normalized to the larger Λ_3 peak) for two values of ξ_i . The optimum value for ξ_i at this photon energy is seen to lie somewhere between the shown values of 0.053 and 0.090. For convenience we shall be using the value of $\xi_i = 0.090$ from here on.

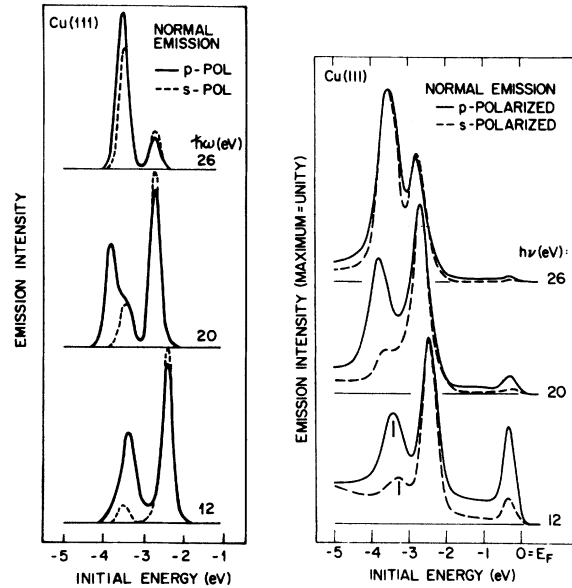


FIG. 3. Theoretical spectra (on the left) are compared with experimental spectra (on the right) showing the differences for s and p polarization. For p polarization a value of $\xi_i = 0.090$ was used.

B. s and p polarization

The different normal photoemission spectra obtained for s - and p -polarized light are compared in Fig. 3 for three photon energies. The agreement between theory and experiment is seen to be quite good. In the case of s -polarized light, only the two Λ_3 bands can be excited. It is seen (dashed curves in Fig. 3) that their relative strengths are well reproduced by the theoretical results; at the lower photon energies, the upper Λ_3 emission peak is more intense; at the highest photon energy, $\hbar\omega = 26$ eV, the lower Λ_3 peak is more intense. This can be traced in Fig. 1 to the k_1 dependence of the momentum matrix elements on approaching the zone center.

For p -polarized light, emission from Λ_1 bands is permitted. Once again, the agreement between theory and experiment is seen to be good. As above, however, this agreement has been obtained by setting $\xi_i = 0.090$, a value much lower than that corresponding to the actual experimental conditions.

C. $\hbar\omega$ dependence

The dependence of the normal photoemission spectra for Cu(111) on photon energy is shown in Fig. 4 for the particularly interesting range $\hbar\omega = 6.0$ – 11.5 eV. The radiation is p polarized, and setting $\xi_i = 0.090$ for the whole range is found to bring about reasonable agreement between theory

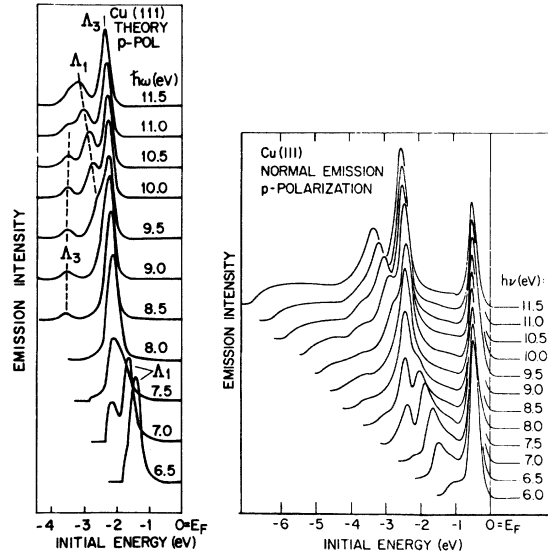


FIG. 4. Photon-energy dependence of the normal photoemission spectra from Cu(111) for p -polarized light. Theoretical spectra (with $\xi_t = 0.090$) on the left are compared with the experimental spectra of Ref. 4 on the right. The intense surface-state emission from just below the Fermi level is, of course, not reproduced by the bulk-band-structure model.

and experiment.

The possibility of finding the optimum value of ξ_t for each individual spectrum, and thereby deriving its $\hbar\omega$ dependence, was considered. This was rendered difficult by the fact that the Λ_1 band crosses the upper Λ_3 band in this photon-energy range and then approaches the lower Λ_3 band (see Fig. 1). A precise determination of the effective ξ_t is further rendered difficult by the possible effects of group velocity and detailed escape considerations on the spectra as one approaches the low photon energies.⁸ For these reasons it was decided to treat ξ_t as a constant over this range, and a value of 0.090 appears to work very well.

IV. LOCAL-FIELD CONSIDERATIONS

The main outcome of the bulk-band calculations performed in this work is that good agreement can be obtained between theory and experiment provided (1) emission from positively identified surface states is ignored, and (2), in the case of p polarization, the value of ξ_t ($= |A_{p\perp}/A_{p\parallel}|^2$ inside the solid) is deliberately suppressed to a lower value. The latter point will now be discussed

Classically, the macroscopic electromagnetic fields inside and outside the solid are determined by the Fresnel equations,⁹ which in turn are based upon Snell's Law,

$$\sin \theta_i = \hat{n} \sin \theta_t. \quad (4)$$

Here θ_t is a complex angle of transmission and \hat{n} ($= n + ik$) is the refractive index of the solid. The quantity ξ_t defined in Eq. (3) is then given by

$$\xi_t \equiv |\tan \theta_t|^2 = \frac{\sin^2 \theta_i}{[(\epsilon_1 - \sin^2 \theta_i)^2 + \epsilon_2^2]^{1/2}}, \quad (5)$$

where $\epsilon_1 + i\epsilon_2 = \hat{n}^2$ is the complex dielectric function. It is convenient to define also a "suppression factor," the factor by which the relative values of $|A_{p\perp}|^2$ and $|A_{p\parallel}|^2$ change on crossing the surface:

$$\xi \equiv \xi_t / \xi_i = |\tan \theta_t / \tan \theta_i|^2 = \frac{\cos^2 \theta_i}{[(\epsilon_1 - \sin^2 \theta_i)^2 + \epsilon_2^2]^{1/2}}. \quad (6)$$

The classical values of ξ and ξ_t are plotted in Figs. 5 and 6 using the known optical constants of copper.¹⁰

The results of Fig. 5 show that for Cu in the range $\hbar\omega < 20$ eV, ξ_t is generally lower than ξ_i . This suppression, due to the macroscopic optical constants, while considerable, is insufficient to account for the very low values of ξ_t needed in the theory to reproduce the experimental spectra (Figs. 2-4). We are therefore obliged to con-

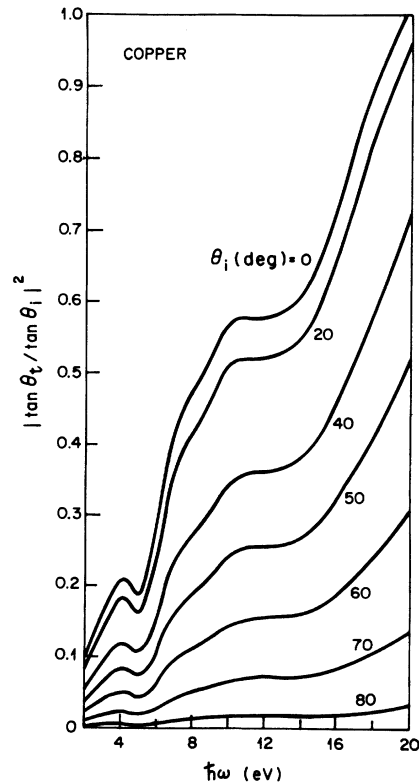


FIG. 5. Dependence of the suppression factor (ξ_t/ξ_i) with $\hbar\omega$ as given by the known optical constants of Cu and the macroscopic Fresnel equations.

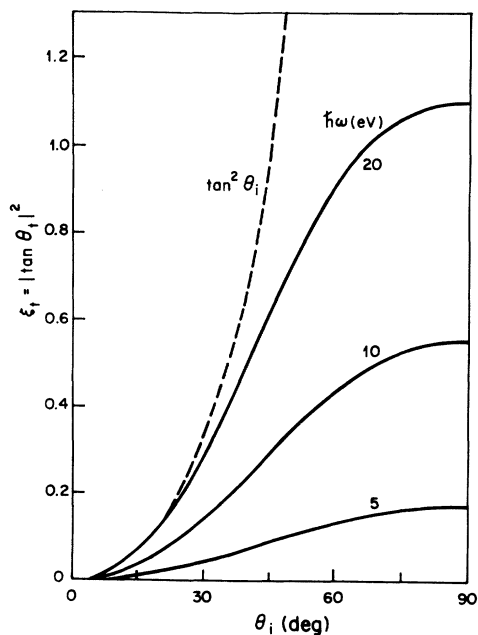


FIG. 6. Dependence of ξ_i (the interior value of $|A_{p\perp}/A_{p\parallel}|^2$) on angle of incidence θ_i calculated using the known optical constants of Cu at three selected photon energies. Note that ξ_i does not increase indefinitely as $\theta_i \rightarrow 90^\circ$ as $\tan^2 \theta_i$ does, but saturates at a maximum value. For $\hbar\omega \lesssim 20$ eV, $|A_{p\perp}|^2$ rarely exceeds $|A_{p\parallel}|^2$, implying that it is impossible to suppress the Λ_3 emission relative to the Λ_1 emission by arbitrarily increasing the angle of incidence.

clude that there is some other source for this suppression. One possibility is that the theoretical calculations are in error; they are, after all, based on a second-principles method for calculating band energies and momentum matrix elements. In response to this, we note that in Ref. 3 the present second-principles approach gave excellent results in the calculation of ϵ_2 (at least in the region $\hbar\omega \lesssim 7$ eV). It therefore seems unlikely that this can account for the major discrepancy (a factor of ~ 5) between the classical Fresnel value of $\xi_i \sim 0.45$ and the value $\xi_i \sim 0.090$ required to produce agreement between theory and experiment. Liebowitz *et al.*¹¹ have also remarked on this suppression effect. Their methods¹² are different from those used here; in particular, the magnitude of the suppression is obscured because it is absorbed to some extent in their empirical parametrization of the momentum matrix element vector. Our method, by contrast, does not require the introduction of any new disposable parameters in the evaluation of the momentum matrix elements.

What, then, is the physical origin of this additional suppression? A possible explanation which comes to hand is that the extra suppression is associated with the local microscopic behavior of the electromagnetic field in the immediate vicinity of the surface. As shown by Feibelman and others,^{13,14} the local field which determines the optical transition strength can depart appreciably from the classical Fresnel values. The departures arise through the need to solve both Maxwell's equations and Schrödinger's equation in a self-consistent manner in the presence of a term of the form $\langle i | \vec{\nabla} \cdot \vec{A} | f \rangle$ which is clearly sensitive to spatial variations of A . We propose, therefore, that the suppression of ξ_i by about a factor of 5, which we have introduced in order to match theory and experiment, is a measure of these local-field effects. There are, however, some objections to this explanation. As shown by Feibelman,¹³ the local-field effects are strongly frequency dependent, whereas we have found that a constant value of ξ_i serves quite well. Further, surface local-field effects occur mostly in the few angstroms nearest the surface. Thus, it is far from obvious that one can simply scale the bulk photoexcitation results by the surface $|A_1|^2$ value.

Another possible explanation is that the discrepancy resides in the form of the wave functions $|i\rangle$ rather than in A . If the initial-state Bloch wave functions increase in amplitude close to the surface (surface resonance), the matrix elements for photoemission should be enhanced. Similarly, if the Bloch functions decrease in amplitude (surface antiresonance), the matrix elements should be depressed. However, there is no support of which we are aware, either theoretical or experimental, for the idea that the Λ_3 levels are resonant or the Λ_1 levels antiresonant at the surface. Also, the Λ_1 band changes character from plane-wave-like to d -like over the photon-energy range of the experiments, so we would once again expect a strong frequency dependence for the effect. Clearly these matters require further investigation. It would be most desirable to perform further calculations for a variety of metals, crystal faces, and directions of emission to first of all test whether the discrepancies are not just an artifact of the second-principles method of calculation.

ACKNOWLEDGMENTS

We are grateful to F. J. Himpsel for providing further details of the experiments of Ref. 4. This work was supported in part by the National Science Foundation through Grant No. DMR-78-11663.

- ¹See, for example, *Photoemission in Solids; Topics in Applied Physics*, edited by M. Cardona and L. Ley (Springer, Berlin, 1978), Vols. I and II.
- ²N. V. Smith and L. F. Mattheiss, *Phys. Rev. B* 9, 1341 (1974); M. M. Traum and N. V. Smith, *ibid.* 9, 1353 (1974); N. V. Smith, *ibid.* 9, 1365 (1974); N. V. Smith, G. K. Wertheim, S. Hufner, and M. M. Traum, *ibid.* 10, 3197 (1974); J. E. Rowe and N. V. Smith, *ibid.* 10, 3207 (1974); N. V. Smith and S. Chiang, *ibid.* 19, 5013 (1979).
- ³N. V. Smith, *Phys. Rev. B* 19, 5019 (1979).
- ⁴J. A. Knapp, F. J. Himpsel, and D. E. Eastman, *Phys. Rev. B* 19, 4952 (1979).
- ⁵E. I. Blount, in *Solid State Physics*, edited by F. Seitz and D. Turnbull (Academic, New York, 1962), Vol. 13, p. 305.
- ⁶See, for example, N. V. Smith in Ref. 1, and W. D. Grobman, D. E. Eastman, and J. L. Freeouf, *Phys. Rev. B* 12, 4405 (1979).
- ⁷F. J. Himpsel, private communication.
- ⁸A simple refinement, but one which was not performed here, would be to multiply the spectra by the "transport factor" of the three-step model which can be approximated by αl , where α is the optical absorption coefficient and l is the hot-electron mean free path; l is given by $v_g \tau$ where v_g is a group velocity readily evaluated from the bands and τ is a lifetime whose dependence on electron energy is well known.
- ⁹M. Born and E. Wolf, *Principles of Optics*, (Pergamon, New York, 1970), p. 615.
- ¹⁰H.-J. Hageman, W. Gudat, and C. Kunz, Deutsches Elektronen-Synchrotron (DESY) special report, 1974 (unpublished).
- ¹¹D. Liebowitz, M. Sagurton, and N. J. Shevchik (unpublished).
- ¹²N. J. Shevchik and D. Liebowitz, *Phys. Rev. B* 18, 1618 (1978); 18, 1630 (1978); M. Sagurton and N. J. Shevchik, *ibid.* 17, 3859 (1978); *J. Phys. C* 11, L353 (1978).
- ¹³P. J. Feibelman, *Phys. Rev. Lett.* 34, 1092 (1975); *Phys. Rev. B* 12, 1319 (1975).
- ¹⁴J. G. Endriz, *Phys. Rev. B* 7, 3464 (1973); K. L. Kliewer, *ibid.* 14, 1412 (1976); 15, 3759 (1977); H. J. Levinson, E. W. Plummer, and P. J. Feibelman, *Phys. Rev. Lett.* 43, 952 (1979).